Bioorganic & Medicinal Chemistry 17 (2009) 1997–2001

Contents lists available at ScienceDirect

Bioorganic & Medicinal Chemistry

journal homepage: www.elsevier.com/locate/bmc

Effects of the introduction of inversion of polarity sites in the quadruplex forming oligonucleotide TGGGT

Veronica Esposito [a], Antonella Virgilio [a], Antonietta Pepe [b], Giorgia Oliviero [a], Luciano Mayol [a], Aldo Galeone [a,*]

[a] Università degli Studi di Napoli Federico II, Dipartimento di Chimica delle Sostanze Naturali, via D. Montesano, 49, 80131 Napoli, Italy
[b] Università degli Studi della Basilicata, Dipartimento di Chimica, via N. Sauro, 85, 85100 Potenza, Italy

ARTICLE INFO

Article history:
Received 30 September 2008
Revised 13 January 2009
Accepted 14 January 2009
Available online 20 January 2009

Keywords:
Quadruplex
Inversion of polarity sites
Glycosidic conformation

ABSTRACT

Insight into the influence of inversion of polarity sites on the structural features of quadruplex structures is presented. The NMR and CD studies concern modified oligodeoxynucleotides (ODNs) based on the quadruplex forming sequence TGGGT. The presence of inversion of polarity sites not only does not compromise the formation of quadruplexes, but in some cases it increases the thermal stability of modified complexes compared with that of the unmodified one.

1. Introduction

Guanine-rich nucleic acid motifs are able to form G-quadruplex structures characterized by a core that is composed of guanines disposed in rotationally symmetric arrangements of four bases, usually called G-quartets or G-tetrads, stabilized by both eight hydrogen bonds and monovalent cations.[1] The biological interest towards these structures is constantly increasing and it is mainly based on three aspects: (i) their presence into the telomeres architectures of several organisms;[2] (ii) the occurrence of many G-rich regulation regions in the human genome;[3] (iii) the aptitude of some aptamers to adopt a G-quadruplex based scaffold.[4]

As it is witnessed by a plethora of scientific reports and some G-quadruplexes classification proposals,[5,6] these structures possess a remarkable structural variability. In fact, they can be different for several structural features that, however, are not independent from each other. For example, three main characteristics, namely the relative strand orientations, the glycosidic conformation (*syn* or *anti*) of the G-residues and the grooves sizes, are mutually interconnected. As a matter of fact, each of the four possible strand arrangements, namely A_4 (all strands parallel), A_3B (three strands parallel and one antiparallel), A_2B_2 (two adjacent strands parallel and the others antiparallel) and $(AB)_2$ (each strand running in the opposite direction respect to the adjacent ones), is characterized by different type of tetrads: all G-*anti* for A_4, *syn–syn–syn–anti* or *anti–anti–anti–syn* for A_3B, *syn–syn–anti–anti* for A_2B_2 and *syn–anti–syn–anti* for $(AB)_2$.[5] Furthermore, the types of tetrads affect the size of the four grooves along the quadruplex structure.[7] The structural variability of G-quadruplexes has been further increased by introducing modification on both bases[8] and sugar-phosphate backbone.[9] In the latter frame, quadruplex structures containing a 3′–3′ or 5′–5′ inversion of polarity site have been described.[10–12] In a G-rich sequence, an inversion of polarity site can be introduced in three different points: into the non-G tract, into the G-tract and just between the two types of tracts. As the first point is concerned, some authors showed that the inversion of polarity site is able to affect the quadruplex strand orientation and, hence, the thermal stability.[12] Interesting results have been obtained from some of us in studying quadruplex structures containing an inversion of polarity site into the G-tracts, namely $^{5'}$TGG$^{3'}$-$^{3'}$GGT$^{5'}$ (Q33), $^{3'}$TGG$^{5'}$-$^{5'}$GGT$^{3'}$ (Q55),[10] $^{5'}$TG$^{3'}$-$^{3'}$GGGT$^{5'}$ (QS33) and $^{3'}$TG$^{5'}$-$^{5'}$GGGT$^{3'}$ (QS55).[11] Among these, Q33 and QS33 show parallel-like quadruplexes, each characterized by four all G-*anti* tetrads. On the other hand, although Q55 maintains a parallel-like structure, it possesses an all G-*syn* tetrad adjacent to the inversion of polarity site, while QS55 shows a twofold symmetric structure in which a tetrameric antiparallel quadruplex is embedded between two parallel tracts.[11]

In order to get further insight into the influence of the inversion of polarity site on the glycosidic conformation of the adjacent G residues, we have undertaken a systematic study based on a series of six oligonucleotides all containing an inversion of polarity site (ODNs **I**–**III** 3′–3′ series and **IV**–**VI** 5′–5′ series in Table 1). Among these, **I** and **IV** also possess an abasic site (dS) replacing a T residue

* Corresponding author. Tel.: +39 081678542; fax: +39 081678552.
E-mail address: galeone@unina.it (A. Galeone).

0968-0896/$ - see front matter © 2009 Elsevier Ltd. All rights reserved.
doi:10.1016/j.bmc.2009.01.027

Table 1
ODNs sequences used in this study and T_m values of quadruplexes formed by them

	Sequence	T_m (°C)
I	$^{5'}$dS$^{3'}$-$^{3'}$GGGT$^{5'}$	39
II	$^{5'}$T$^{3'}$-$^{3'}$GGGT$^{5'}$	44
III	$^{5'}$TG$^{3'}$-$^{3'}$GGT$^{5'}$	49
IV	$^{3'}$dS$^{5'}$-$^{5'}$GGGT$^{3'}$	39
V	$^{3'}$T$^{5'}$-$^{5'}$GGGT$^{3'}$	45
VI	$^{3'}$TG$^{5'}$-$^{5'}$GGT$^{3'}$	72

The underlined residues indicate a *syn* glicosidic conformation. The abasic site is indicated by dS (dSpacer, see Fig. 1).

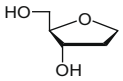

Figure 1. Structure of dSpacer (dS) introduced in ODNs **I** and **IV** as abasic site.

at one sequence end (Fig. 1). The nature and the thermal stability of the quadruplexes adopted by them have been investigated by NMR and CD methods.

2. Results and discussion

ODNs **I**–**VI** were synthesized through the standard phosphoramidite chemistry by using normal 3′-phosphoramidites for the 3′–5′ tracts and 5′–phosphoramidites for the 5′–3′ tracts. For ODNs **I**–**III**, an universal support was also exploited, while 5′-dimethoxytrityl protected 3′-phosphoramidite 1′,2′-dideoxyribose (labelled dSpacer: dS in Table 1) was employed for ODNs **I** and **IV** with the aim of introducing an abasic site in the sequences.

In order to assess the ability of ODNs **I**–**VI** to fold in quadruplex structures and, in case, to establish their nature, we mainly used NMR experiments. Thus, NMR samples of ODNs **I**–**VI** were prepared at a concentration of approximately 3 mM, in 0.6 mL (H_2O/D_2O 9:1) buffer solution having 10 mM KH_2PO_4, 70 mM KCl, 0.2 mM EDTA, pH 7.0. One of the defining features of structures containing G-tetrads is the appearance of imino proton resonances in the region between 10.5 and 12.0 ppm in NMR spectra.[13] Examination of this region is generally used to assess whether the sequence adopts a unique structure. For each ODN under investigation, three main signals are clearly evident in the diagnostic region of the ^{1}H NMR spectra, thus indicating the presence of three imino protons involved in Hoogsteen hydrogen bonds belonging to a major conformation (Fig. 2), although small peaks suggest the presence of other minor conformations in slow equilibrium, as well. Since each of the ODNs **I**–**VI** contains three G-residues in its sequence, the resulting quadruplex structures possess a fourfold symmetry (C_4). Most of the ^{1}H NMR resonances have been assigned by means of the analysis of 2D TOCSY and 2D NOESY experiments (see Supplementary data). The NOE patterns of 5′–3′ and 3′–5′ tracts for ODNs **I**–**III** (3′–3′ series) turned out to be similar to that of the corresponding tracts in $^{5'}$TGG$^{3'}$-$^{3'}$GGT$^{5'}$ (Q33)[10] and $^{5'}$TG$^{3'}$-$^{3'}$GGGT$^{5'}$ (QS33).[11] Moreover, the entire path of NOE connectivities observed for all Gs indicates that the backbone conformation resembles that of the unmodified [d(TGGGT)]$_4$,[14] possessing a right-handed helix structure. For each ODNs **I**–**III**, the lack of strong NOEs between any G H8 and H1′ of the same residue, in comparison to those observed between each G H8 and its ribose H2′/H2″, indicates that all G residues are in the *anti* glycosidic conformation (for an example see Fig. 3). The whole of the data concerning the 3′–3′ ODNs series strongly suggests that each of them adopts a parallel-like quadruplex structure in which the 3′–3′ inversion of polarity sites are approximately in the same position along the complex and all G residues adopt *anti* glycosidic conformations (Fig. 4A).

As far as ODNs **IV**–**VI** (5′–5′ series) are concerned, their behaviour turned out to be less uniform compared to that of the 3′–3′ ODNs series. Indeed, an in-depth analysis of the 2D NOESY spectrum of quadruplexes formed by **V** and **VI**, clearly point out intense intraresidual H8–H1′ NOEs (diagnostic of a *syn* glycosidic conformation) (Fig. 5B and C). The entire set of NOE crosspeaks allowed us to assign these signals to the first G residue of the $^{5'}$GGGT$^{3'}$ (**V**) and $^{5'}$GGT$^{3'}$ (**VI**) tracts. In both cases the all-*syn* tetrads are adjacent to the 5′–5′ inversion of polarity site. In agreement with literature data, the H8 resonance of these *syn* G residues is upfield shifted with respect to those of the *anti* ones.[11] On the other hand, the behaviour of **IV** in solution was significantly different from those of **V** and **VI**, notwithstanding **IV** belongs to the 5′–5′ series. In fact, no strong NOE between any G H8 and H1′ of the same residue could be observed in its 2D NOESY spectrum, thus indicating that all G residues adopt an *anti* glycosidic conformation (Fig. 5A). According to the data reported above, we propose that ODNs **IV**–**VI** adopt the quadruplex structures showed in Figure 4B. For the 5′–5′ series, the whole of collected NMR data suggests that a 5′–5′ inversion of polarity site is able to promote the formation of an adjacent all-*syn* G-tetrad on condition that the flanking 5′ residue is not an abasic one. As a matter of fact, the crucial role of the base flanking the 5′–5′ inversion of polarity site clearly comes out in **IV** since this possesses a sugar-mimic moiety (dSpacer) next to the 5′–5′

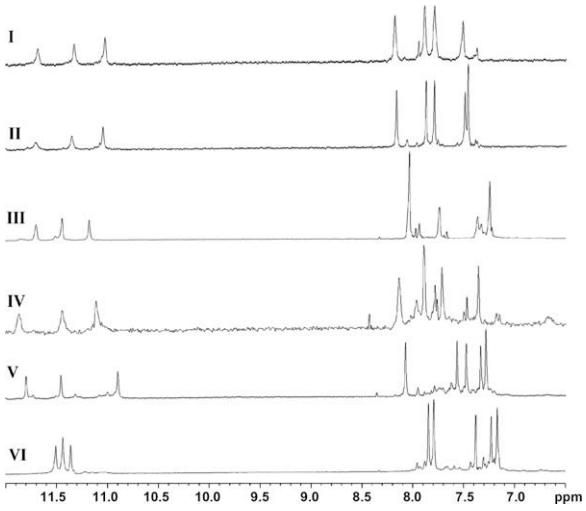

Figure 2. Selected region of the ^{1}H NMR spectra of ODNs **I**–**VI**. The guanine imino protons involved in G-tetrad formation resonate between 10.5 and 11.5 ppm. The narrow non-exchangeable base protons resonate between 7.0 and 8.5 ppm.

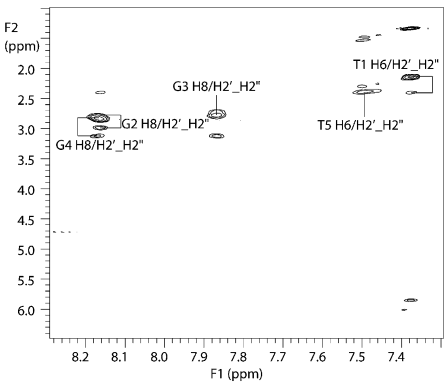

Figure 3. 2D-NOESY (500 MHz, 180 ms, T = 25 °C) contour plots correlating base H8/H6 and sugar H2′/H2″ protons in **III**.

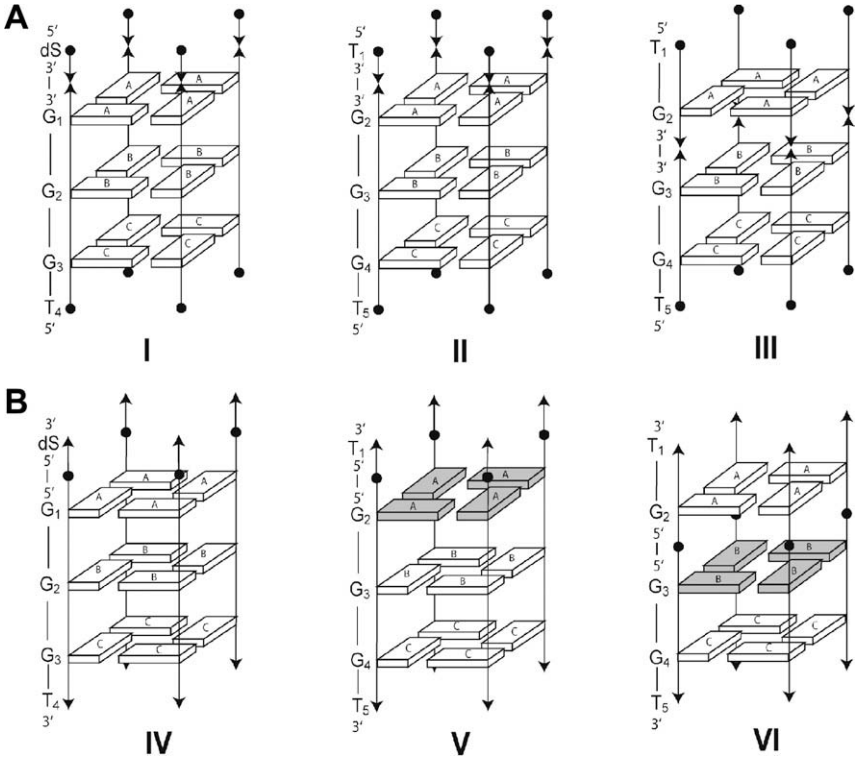

Figure 4. Schematic illustration of the quadruplex structures formed by ODNs **I**–**VI** (**A**: 3′–3′ series; **B**: 5′–5′ series). Black arrowheads and circles indicate 3′ and 5′ edges of each subunit/strand, respectively. The *anti* and *syn* guanines are depicted as white and gray solids, respectively. For each structure, equivalent guanines are indicated by the same letter.

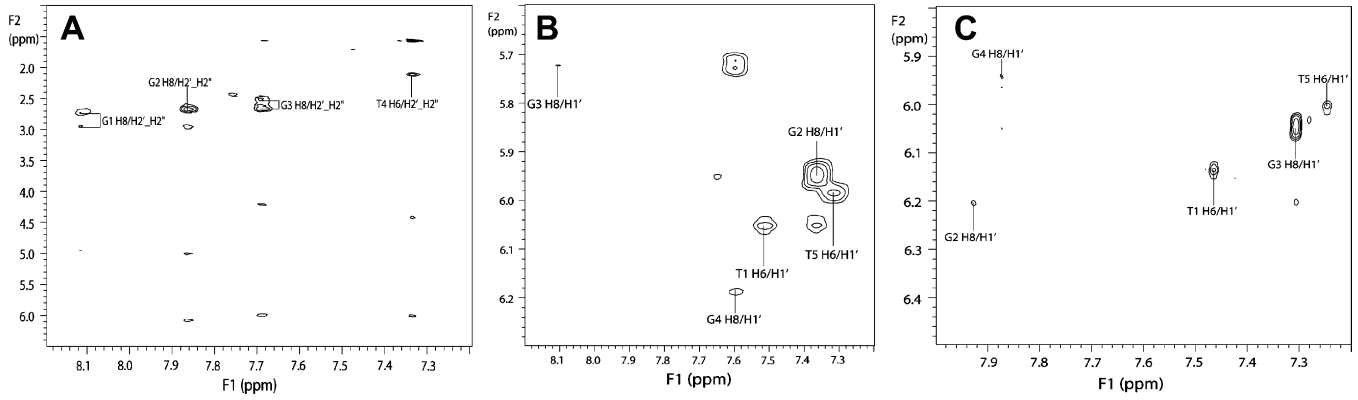

Figure 5. 2D-NOESY (500 MHz, 180 ms, $T = 25$ °C) contour plots correlating base H8/H6 and sugar H2′/H2″ protons in **IV** (A) and base H8/H6 and sugar H1′ protons in **V** (B) and **VI** (C).

inversion of polarity site replacing a nucleoside and it forms a quadruplex only containing *anti* dG residues, although a 5′–5′ inversion of polarity site is present.

Circular dichroism is a technique often used to get preliminary information about the quadruplex folding topology. Generally, parallel quadruplexes, in which the glycosidic bonds are all *anti*, display a positive CD signal around 265 nm, with a negative peak at 240 nm.[15] On the contrary, antiparallel strands arrangements containing both *syn* and *anti* glycosidic bonds, exhibit a positive signal at around 295 nm, with a negative signal or shoulder around 260 nm. CD spectra of quadruplexes formed by ODNs **I**–**VI** and their natural counterpart $[d(TGGGT)_4]$[14] were acquired at 20 °C and are reported in Figure 6. All the measurements were performed at a concentration of 1×10^{-4} M in the potassium buffer used for NMR experiments. CD spectra of **I**, **II**, **IV** and $[d(TGGGT)_4]$ are very similar and confirm results obtained by NMR experiments, pointing to parallel-like quadruplex structures all containing only *anti* G residues. Although, according to NMR data, also **III** shows a parallel-like structure, its CD spectrum comes out different from the typical spectrum of a parallel quadruplex. As a matter of fact, it shows two positive bands at 249 and 294 and two negative bands at 230 and 265 nm, respectively.

However, this should not be considered particularly surprising taking into account the presence of a 3′–3′ inversion of polarity site into the G-tract, that alters the standard tetrads stacking typical of a parallel quadruplex. In this respect, the CD spectrum of **III** matches those of its homologous quadruplexes formed by ODNs $^{5'}TGG^{3'}$-$^{3'}GGT^{5'}$ (Q33)[10] and $^{5'}TG^{3'}$-$^{3'}GGGT^{5'}$ (QS33)[11] in which similar bands and values have been observed. As for CD spectra of **V** and **VI**, their profiles are quite different from the other ones reflecting the differences in the quadruplex structures. The CD spectrum of **V** displays a negative band at 233 nm and two positive bands at

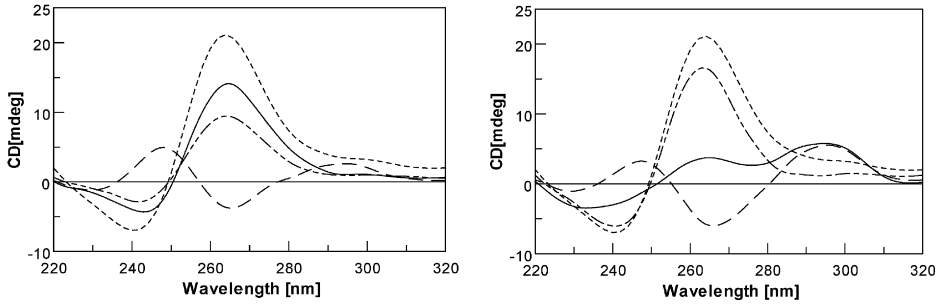

Figure 6. CD spectra of ODNs **I** (---), **II** (—), **III** (——) (left) and ODNs **IV** (---), **V** (—), **VI** (— —) (right) compared with their natural counterpart [d(TGGGT)$_4$] (---).

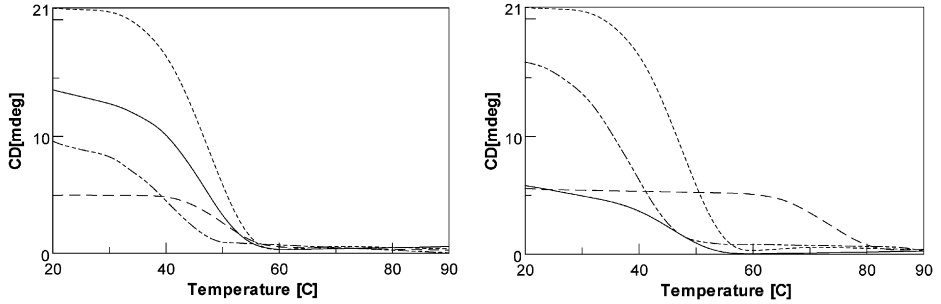

Figure 7. CD melting profiles of ODNs **I** (---), **II** (—), **III** (——) (left) and ODNs **IV** (---), **V** (—), **VI** (——) (right) compared with their natural counterpart [d(TGGGT)$_4$] (---).

265 and 295 nm. As above reported, the latter one is typical of quadruplex structures containing both *syn* and *anti* G-residues. On the other hand, the CD spectrum of **VI** shows two positive bands at 247 and 296 and two negative bands at 229 and 266 nm, respectively, once again confirming the presence of *syn* and *anti* G-residues. Furthermore, its CD spectrum closely matches that of the quadruplex formed by $^{3'}$TGG$^{5'}$-$^{5'}$GGT$^{3'}$ (Q55)[10] in which a similar strands arrangement and an all G-*syn* tetrad occur.

In order to estimate thermal stability of structures formed by **I**–**VI**, each ODN was subjected to melting and annealing CD measurements in comparison with [d(TGGGT)$_4$] under the same experimental conditions. All experiments were performed at a concentration of 1×10^{-4} M using potassium buffer. As expected, due to the tetramolecular nature of the complexes, severe hysteresis phenomena were observed for all ODNs (data not shown), despite the very slow scan rates used (10 °C h^{-1}), thus indicating that the systems were not at equilibrium. However, we obtained good melting profiles (Fig. 7) that allowed us to determine the apparent melting temperature (T_m) usually considered quite useful to compare thermal stabilities. The apparent melting temperatures of ODNs **I**–**VI** were listed in Table 1.

Regarding the 3′–3′ series, the comparison between T_m of **I** (39 °C) and **II** (44 °C) point towards a positive contribution of the thymine base to the complex stability, since in **I** an abasic site adjacent to the 3′–3′ inversion replaces the T base in the sequence. Furthermore the T_m of **II** is comparable to that of its natural counterpart [d(TGGGT)$_4$] (45 °C), thus indicating that, in this case, the influence of the 3′–3′ inversion of polarity site on quadruplex stability can be considered negligible. Very similar observations can be made for the corresponding ODNs of the 5′–5′ series (**IV** and **V**), despite the fact that, differently from the previous complexes, **V** adopts a quadruplex in which an all G-*syn* tetrad occurs. Interesting results concern T_m of ODNs **III** and **VI** that turned out to be more stable than their natural counterpart, notwithstanding the inversion of polarity sites are incorporated in the G-tracts. Particularly interesting is the thermal stability of quadruplex **VI** (72 °C) in which, not only the presence of an all G-*syn* tetrad in the G-tracts is well tolerated, but it seems to cause a remarkable enhancement in apparent T_m (about 27 °C) compared with that of their natural counterpart, similar to that observed between the homologous quadruplexes formed by $^{3'}$TGG$^{5'}$-$^{5'}$GGT$^{3'}$ (Q55)[9] and d(TGGGGT)[14] (about 25 °C).

3. Conclusion

Results reported here allowed to reach several conclusions. Taking into account similar studies devoted to the sequence TGGGGT,[10,11] it has been confirmed that in parallel-like quadruplex structures, a 5′–5′ inversion of polarity site is able to favour the formation of an adjacent all-*syn* G-tetrad. However, the role of the other base adjacent to the inversion point should be taken in consideration as well, since an abasic site in this position has turned out unable to induce an all-*syn* G-tetrad arrangement. At the best of our knowledge, all-*syn* G-tetrads have been induced in quadruplex structures only by using modified guanines[16] or in complexes formed by the self-assembly of lipophilic guanosine derivatives.[17] The introduction of an all-*syn* G-tetrad comes out potentially useful in post-SELEX modifications of quadruplex based aptamers in which the interaction with the target could be improved by the fine tuning of the local groove size and the orientation of the 2-amino group as hydrogen bond donor. It should be noted that an inversion of polarity site has already been successfully introduced into an anti-VEGF aptamer, namely Macugen (Pegaptanib), that has been recently approved by the USA FDA for the treatment of neovascular age-related macular degeneration.[18] In general, the presence of an inversion of polarity site increases the stability of oligonucleotides towards the hydrolytic action of nucleases and this feature is fundamental in view of the potential use in vivo of an ODN aptamer. The effect of the presence of inversion of polarity sites on thermal stability is a further feature that has been investigated in this study. Although we could give an only qualitative evaluation, the introduction of a 5′–5′ inversion of polarity site into the G-tract of the sequence TGGGT clearly points towards a remarkable enhancement of the thermal stability in comparison

with their natural counterpart. This aspect could be undoubtedly appealing in the design of new aptamers or in the properties tuning of biologically active aptamers (for example anti-HIV ODNs including sequence TGGG),[19] particularly taking into account the relatively reduced size of the quadruplex structure in which the thermal stability improvement has been obtained.

4. Experimental

4.1. Oligonucleotides synthesis

The oligonucleotides **I**–**VI** were synthesized on a Millipore Cyclone Plus DNA synthesizer using solid phase β-cyanoethyl phosphoramidite chemistry at 15 μmol scale. The synthesis of the 3′–5′ tracts were performed by using normal 3′-phosphoramidites, whereas the 5′–3′ tracts were synthesized by using 5′-phosphoramidites. For ODNs **I**–**III**, an universal support was also used. The introduction of an abasic site in **I** and **IV** was performed by using 5′-dimethoxytrityl-3′-phosphoramidite-1′,2′-dideoxyribose (dSpacer, Link Technologies). The oligomers were detached from the support and deprotected by treatment with concentrated aqueous ammonia at 80 °C overnight. The combined filtrates and washings were concentrated under reduced pressure, redissolved in H_2O, analyzed and purified by high-performance liquid chromatography (HPLC) on a Nucleogel SAX column (Macherey–Nagel, 1000-8/46); using buffer A: 20 mM KH_2PO_4/K_2HPO_4 aqueous solution (pH 7.0), containing 20% (v/v) CH_3CN; buffer B: 1 M KCl, 20 mM KH_2PO_4/K_2HPO_4 aqueous solution (pH 7.0), containing 20% (v/v) CH_3CN; a linear gradient from 0% to 100% B for 30 min and flow rate 1 mL/min were used. The fractions of the oligomers were collected and successively desalted by Sep-pak cartridges (C-18). The isolated oligomers proved to be >98% pure NMR.

4.2. Nuclear magnetic resonance experiments

NMR samples were prepared at a concentration of ~3 mM, in 0.6 mL (H_2O/D_2O 9:1 v/v) buffer solution having 10 mM KH_2PO_4/K_2HPO_4, 70 mM KCl and 0.2 mM EDTA (pH 7.0). For D_2O experiments, the H_2O was replaced with D_2O by drying down the sample, lyophilization and redissolution in D_2O alone. NMR spectra were recorded with a Varian Unity INOVA 500 MHz spectrometer. ^1H chemical shifts were referenced relative to external sodium 2,2-dimethyl-2-silapentane-5-sulfonate (DSS). 1D proton spectra of samples in H_2O were recorded using pulsed-field gradient WATERGATE[20] for H_2O suppression. Phase sensitive NOESY spectra[21] were recorded with mixing times of 80 and 180 ms (T = 25 °C). Pulsed-field gradient WATERGATE was used for NOESY spectra in H_2O with 200 ms mixing times. TOCSY spectra[22] with mixing times of 120 ms were recorded with D_2O solutions. NOESY and TOCSY were recorded using a TPPI[23] procedure for quadrature detection. In all 2D experiments the time domain data consisted of 2048 complex points in $t2$ and 400–512 fids in $t1$ dimension. The relaxation delay was kept at 1.2 s for all experiments.

4.3. Circular dichroism

CD samples of **I**–**VI**, and their natural counterpart $[d(TGGGT)]_4$ were prepared at a concentration of 1×10^{-4} M by using the buffer solution used for NMR experiments: 10 mM KH_2PO_4/K_2HPO_4, 70 mM KCl and 0.2 mM EDTA (pH 7.0). CD spectra of all quadruplexes and CD melting curves were registered on a Jasco 715 CD spectrophotometer. For the CD spectra, the wavelength was varied from 220 to 320 nm at 100 nm min^{-1} scan rate, and the spectra recorded with a response of 16 s, at 2.0 nm bandwidth and normalized by subtraction of the background scan with buffer. The temperature was kept constant at 20 °C with a thermoelectrically-controlled cell holder (Jasco PTC-348). CD melting curves were registered as a function of temperature from 20 to 90 °C for all quadruplexes at their maximum Cotton effect wavelengths. The CD data were recorded in a 0.1 cm pathlength cuvette with a scan rate of 10 °C h^{-1}.

Acknowledgments

This work was supported by Italian M.U.R.S.T. (P.R.I.N. 2005 and 2006) and Regione Campania (L.41, L.5). The authors are grateful to 'Centro di Servizio Interdipartimentale di Analisi Strumentale', C.S.I.A.S., for supplying NMR facilities. The authors are also grateful to Adele Alagia, Giuseppe Citarella, Luisa Cuorvo and Pasquale Paciello for their collaboration.

Supplementary data

Supplementary data associated with this article can be found, in the online version, at doi:10.1016/j.bmc.2009.01.027.

References and notes

1. Burge, S.; Parkinson, G.; Hazel, P.; Todd, A. K.; Neidle, S. *Nucleic Acids Res.* **2006**, *34*, 5402.
2. Oganesian, L.; Bryan, T. M. *BioEssays* **2007**, *29*, 155 and references cited therein.
3. Huppert, J. In *Quadruplex Nucleic Acids*; Neidle, S., Balasubramanian, S., Eds.; RSC Publishing: London, 2006, Chapter 8, pp 208–227 and references cited therein.
4. (a) Chou, S.-H.; Chin, K.-H.; Wang, A. H.-J. *Trends Biochem. Sci.* **2005**, *30*, 231; (b) Wang, K. Y.; McCurdy, S.; Shea, R. G.; Swaminathan, S.; Bolton, P. H. *Biochemistry* **1993**, *32*, 1899.
5. Esposito, V.; Galeone, A.; Mayol, L.; Oliviero, G.; Virgilio, A.; Randazzo, L. *Nucleosides, Nucleotides Nucleic Acids* **2007**, *26*, 1155.
6. Webba da Silva, M. *Chem. Eur. J.* **2007**, *13*, 9738.
7. Phan, T.; Kuryavyi, V.; Luu, K. N.; Patel, D. J. In *Quadruplex Nucleic Acids*; Neidle, S., Balasubramanian, S., Eds.; RSC Publishing: London, 2006, Chapter 3, pp 81–99 and references cited therein.
8. For a recent example see: Gros, J.; Rosu, F.; Amrane, S.; De Cian, A.; Gabelica, V.; Lacroix, L.; Mergny, J.-L. *Nucleic Acids Res.* **2007**, *35*, 3064.
9. (a) Datta, B.; Bier, M. E.; Roy, S.; Armitage, B. A. *J. Am. Chem. Soc.* **2005**, *127*, 4199; (b) Nielsen, J. T.; Arar, K.; Petersen, M. *Nucleic Acids Res.* **2006**, *34*, 2006.
10. Esposito, V.; Virgilio, A.; Randazzo, A.; Galeone, A.; Mayol, L. *Chem. Commun.* **2005**, 3953.
11. Galeone, A.; Mayol, L.; Virgilio, A.; Virno, A.; Randazzo, A. *Mol. BioSyst.* **2008**, *4*, 426.
12. Martino, L.; Virno, A.; Randazzo, A.; Virgilio, A.; Esposito, V.; Giancola, C.; Bucci, M.; Cirino, G.; Mayol, L. *Nucleic Acids Res.* **2006**, *34*, 6653.
13. Feigon, J.; Koshlap, K. M.; Smith, F. W. *Methods Enzymol.* **1995**, *261*, 225.
14. Renzhe, J.; Gaffney, B. L.; Wang, C.; Jones, R. A.; Breslauer, K. J. *Proc. Natl. Acad. Sci. U.S.A.* **1992**, *89*, 8832.
15. (a) Lu, M.; Guo, Q.; Kallenbach, N. R. *Biochemistry* **1992**, *31*, 2455; (b) Balagurumoorthy, P.; Brahmachari, S. K.; Mohanty, D.; Bansal, M.; Sasisekharan, V. *Nucleic Acids Res.* **1992**, *20*, 4061; (c) Balagurumoorthy, P.; Brahmachari, S. K. *J. Biol. Chem.* **1994**, *269*, 21858.
16. (a) Virgilio, A.; Esposito, V.; Randazzo, A.; Mayol, L.; Galeone, A. *Nucleic Acids Res.* **2005**, *33*, 6188; (b) Esposito, V.; Randazzo, A.; Piccialli, G.; Petraccone, L.; Giancola, C.; Mayol, L. *Org. Biomol. Chem.* **2004**, *2*, 313.
17. (a) Liu, X.; Kwan, I. C. M.; Wang, S.; Wu, G. *Org. Lett.* **2006**, *8*, 3685; (b) Davis, J. T.; Spada, G. P. *Chem. Soc. Rev.* **2007**, *36*, 296.
18. Ng, E. W. M.; Shima, D. T.; Calias, P.; Cunningham, E. T., Jr.; Guyer, D. R.; Adamis, A. P. *Nat. Rev. Drug Discov.* **2006**, *5*, 123.
19. (a) Koizumi, M.; Kaneko, M.; Ohmine, T.; Furukawa, H.; Nishigaki, T. PCT Int. Appl., CODEN: PIXXD2 WO 9919474 A1 19990422, 1999.; (b) Koizumi, M.; Kaneko, M.; Ohmine, T.; Furukawa, H.; Nishigaki, T. PCT Int. Appl., CODEN: PIXXD2 WO 9921874 A1 19990506, 1999.; (c) Koizumi, M.; Kaneko, M.; Ohmine, T.; Furukawa, H.; Nishigaki, T. PCT Int. Appl., CODEN: JKXXAF JP 2000290185 A 20001017, 2000.
20. Piotto, M.; Saudek, V.; Sklenar, V. J. *J. Biomol. NMR* **1992**, *2*, 661.
21. Jeener, J.; Meier, B.; Bachmann, H. P.; Ernst, R. R. *J. Chem. Phys.* **1979**, *71*, 4546.
22. Braunschweiler, L.; Ernst, R. R. *J. Magn. Reson.* **1983**, *53*, 521.
23. Marion, D.; Wuthrich, K. *Biochem. Biophys. Res. Commun.* **1983**, *113*, 967.